

Observation of localized modes at phase slips in two-dimensional photonic lattices

Alexander Szameit¹, Mario I. Molina^{2,3}, Matthias Heinrich⁴

Felix Dreisow⁴, Robert Keil⁴, Stefan Nolte⁴, and Yuri S. Kivshar⁵

¹*Solid State Institute and Physics Department, Technion, 32000 Haifa, Israel*

²*Departamento de Física, Facultad de Ciencias, Universidad de Chile, Santiago, Chile*

³*Center for Optics and Photonics, Universidad de Concepción, Casilla 4016, Concepción, Chile*

⁴*Institute of Applied Physics, Friedrich-Schiller-Universität Jena, Max-Wien-Platz 1, 07743 Jena, Germany*

⁵*Nonlinear Physics Center, Research School of Physics and Engineering, Australian National University, Canberra ACT 0200, Australia*

We study experimentally light localization at phase-slip waveguides and at the intersection of phase-slips in a two-dimensional (2D) square photonic lattice. Such system allows to observe a variety of effects, including the existence of spatially localized modes for low powers, the generation of strongly localized states in the form of discrete bulk and surface solitons, as well as a crossover between one-dimensional (1D) and 2D localization.

The study of nonlinear dynamics in waveguide arrays and photonic lattices has attracted a great deal of attention due to the possibility to observe many novel effects of nonlinear physics and possible interesting applications in photonics [1]. In particular, it was shown that discrete nonlinear photonic systems can support different types of spatially localized states in the form of discrete solitons [2]. These solitons can be controlled by the insertion of suitable defects in an array, as was suggested theoretically [3] and also verified experimentally for arrays of optical waveguides [4]. Defects may provide an additional physical mechanism for light confinement, and they can support spatially localized modes, which have been studied theoretically for different linear [5] and nonlinear [6–8] models and observed experimentally in 1D [5, 9] and 2D [10] photonic lattices.

Recently, a novel type of nonlinear mode has been introduced [11, 12] at the interface between two spatially shifted nonlinear waveguide arrays. These defect modes are closely linked with the phase-slip defects in 2D photonic crystals [13]. In the presence of a phase-slip, the distance between two lattice sites located at both sides of the phase-slip is a non-integer multiple of the lattice constant. As a result, the nonlinear phase-slip defect modes possess the specific properties of both discrete nonlinear surface modes and bulk solitons.

In this Letter we study experimentally, for the first time to our knowledge, light localization in a 2D square photonic lattice containing one phase-slip defect or an intersection of two phase-slip defects. We observe a variety of novel effects, including linear modes localized at the cross intersection of the phase-slips [13], strongly nonlinear localized states in the form of discrete solitons at a single slip [11], and discrete surface solitons at the lattice edges [12]. We also observe and discuss a crossover between 1D and 2D localization.

The considered system consists of an array of $N \times N$ nonlinear focussing (Kerr) waveguides, originally forming a square lattice with periodicity a . Breaking the translational symmetry of the system by altering the distance between two consecutive rows or columns creates a

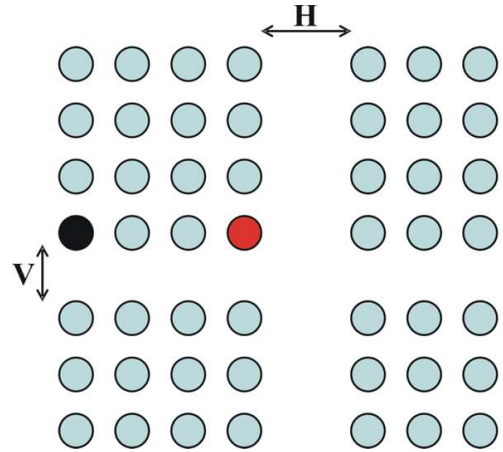


FIG. 1: (Color online) Schematics of an intersection of two different phase slips ($H, V \neq a$). The case of a single phase slip corresponds to either $H \neq a$ or $V \neq a$. Marked waveguides show the excitation points.

phase defect or a cross intersection of two phase-slips (see Fig. 1). The coupling across the defect in the x-direction (y-direction) is termed C_H (C_V). In the framework of the couple-mode theory, the evolution equations for the electric field amplitudes $E_n(z)$ can be written in the form,

$$i \frac{dE_n}{dz} + \sum_m C_{n,m} E_m + \gamma |E_n|^2 E_n = 0 \quad (1)$$

where $E_n(z)$ is the electric field (in units of $(\text{Watt})^{1/2}$) on waveguide n at distance z (in meters), $C_{n,m}$ is the coupling coefficient (in units of $1/\text{meter}$) between guides n and m , and γ (in units of $1/(\text{Watt} \times \text{meter})$) is the nonlinear coefficient, defined by $\gamma = \omega_0 n_2 / c A_{\text{eff}}$, where ω_0 is the angular frequency of light, n_2 is the nonlinear refractive index of the guide and A_{eff} is the effective area of the linear modes. Equation (1) is normalized by defining a dimensionless distance $s \equiv Cz$, where C is the coupling between nearest-neighbor guides outside the vicinity of the slip defect, and the dimensionless electric field

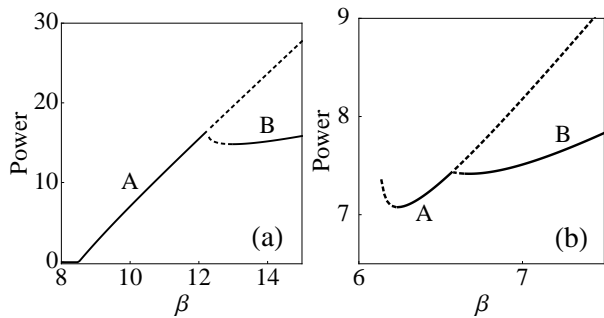


FIG. 2: Power diagrams for the cases: (a) The mode is localized at a cross intersection of two phase slips with $V = H = 29 \mu\text{m}$. (b) Surface mode localized at a single phase slip with $V = 25 \mu\text{m}$, $H = a = 40 \mu\text{m}$. Solid lines refer to stable states while dashed branches refer to the unstable modes.

$\phi_n = (\gamma/C)^{1/2} E_n$. With the above definitions, the conserved power (in Watts) is given by $\sum_n |E_n|^2 = (C/\gamma) P$, where $P \equiv \sum_n |\phi_n|^2$ is the dimensionless power. As was first shown by Apalkov and Raikh [13], a topological defect created by the intersection of two phase-slips, can

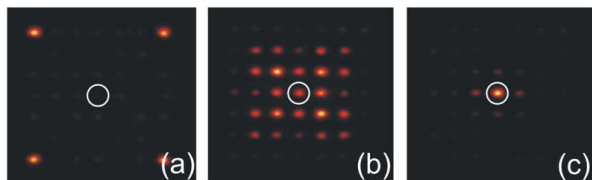


FIG. 3: (Color online) Light diffraction and localization in a perfect square lattice, for different input powers: (a) 75 kW, (b) 1600 kW, and (c) 2000 kW. Excited waveguides are marked with white circles.

support a *linear* localized mode. Looking for stationary *linear* modes ($\gamma = 0$) of the system (1) in the form, $\phi_n(s) = \phi_n \exp(i\beta s)$, we find a linear localized mode at a fixed value of the propagation constant,

$$\beta = C_V + \frac{1}{C_V} + C_H + \frac{1}{C_H}, \quad (2)$$

provided $C_V > 1$ and $C_H > 1$. In the nonlinear case, we follow the recent theoretical results [11, 12] and demonstrate that nonlinearity can support a variety of localized modes including the modes which bifurcate from the symmetric states and describe nonlinear asymmetric localized states. The corresponding bifurcation diagram of low-power branches of localized modes is shown in Figs. 2(a,b) for bulk and surface modes, respectively. When the mode power grows, the symmetric mode A described in the anti-continuum limit by the pattern $\begin{pmatrix} + & + \\ + & + \end{pmatrix}$ becomes unstable, and it transforms into the asymmetric mode B with the pattern $\begin{pmatrix} + & 0 \\ 0 & 0 \end{pmatrix}$ corresponding to the lower bifurcation branch in Fig. 2(a). Similarly, the surface symmetric mode $\begin{pmatrix} + \\ + \end{pmatrix}$ bifurcates into the asymmetric mode $\begin{pmatrix} + \\ 0 \end{pmatrix}$ above a certain power threshold, as shown in

Fig. 2(b). Whereas in the case of Fig. 2(a), the localized modes extend toward vanishing powers, a finite threshold power is required to generate a surface mode in the case of Fig. 2(b).

For the fabrication, we employ the femtosecond direct-writing technique [14]. The specific fabrication parameters can be found, e.g., in [15]. Each array is 100 mm long and consists of 7×7 waveguides, as shown in Fig. 1(a). The spacing between the individual lattice sites is $a = 40 \mu\text{m}$ except in the phase-slip channels, where the spacing is decreased. In the experiments, light of a Ti:sapphire chirped pulse amplification laser system (RegA, Coherent), with a pulse duration of about 180 fs and a repetition rate of 150 kHz at 800 nm, was coupled into the central guide using a $4 \times$ microscope objective [numerical aperture (NA) of 0.1], coupled out by a $10 \times$ objective (NA = 0.25), and projected onto a CCD camera.

First, we study the light propagation in a perfect lattice $V = H = a = 40 \mu\text{m}$. Figures 3(a-c) show the experimental images of the light at the lattice output for different input powers. In the linear regime [Fig. 3(a)], we observe strong discrete diffraction but, when the input power grows, the diffraction is suppressed [Fig. 3(b)], and the generation of a discrete 2D soliton [16] is observed for the input power of 2000 kW [Fig. 3(c)].

Next, we consider a symmetric cross-intersection of two

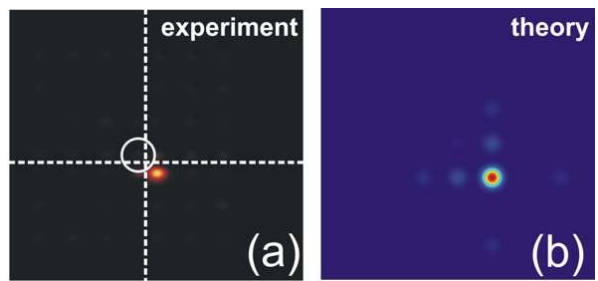


FIG. 4: (Color online) (a) Experimental and (b) Theoretical results for the generation of a linear localized mode at an intersection of two phase-slip waveguides for $V = H = 22 \mu\text{m}$ and an input power 75 kW [cf. Fig. 3(a)]. Excited waveguides are marked with white circles; phase slips are marked by dashed lines.

phase-slip waveguides with the parameters $V = H = 22 \mu\text{m}$, and excite one of the waveguides near the cross, as marked in Fig. 1. Even for a power level as low as 75 kW we observe, in a sharp contrast with the diffraction pattern of Fig. 3(b), the generation of a linear mode localized at the phase-slip intersection. Figures 4(a,b) show both experimental and numerical images of the light intensity at the output facet that confirm the generation of a strongly localized state at the phase-slip defect, in accord with the theory [13]. Because we excite only one site of the lattice, the resulting four-site mode can not be generated as a stationary mode, but it is clearly seen how the light is bound to the phase-slip, which is reproduced by direct numerical simulations, see Fig. 4(b).

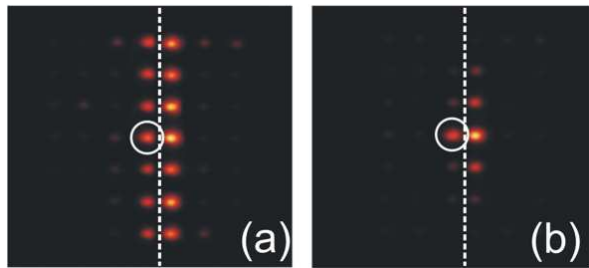


FIG. 5: (Color online) Experimental images of the light intensity at the output facet showing the generation of (a) a 1D stripe surface soliton for an input power 1700 kW, and (b) its transformation into a 2D soliton at 2000 kW. The waveguide parameters are: for $H = 29 \mu\text{m}$, $V = a = 40 \mu\text{m}$. Excited waveguides are marked with white circles; phase slips are marked by dashed lines.

For the next series of experiments, we fabricate a single phase slip and excite one of the central

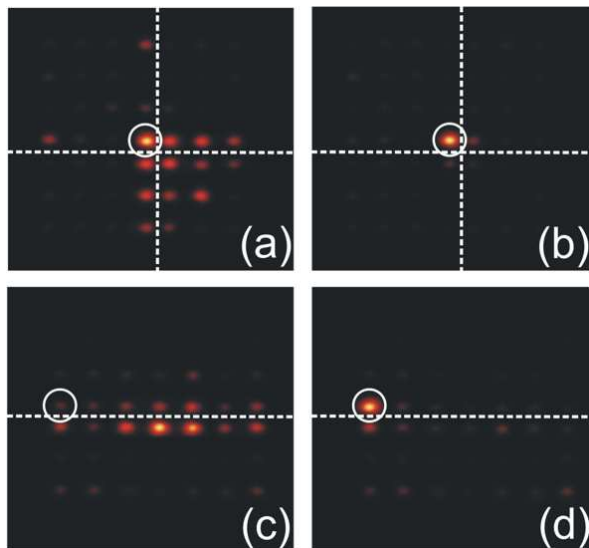


FIG. 6: (Color online) Experimental images of the output light intensity showing the generation of (a,b) 2D soliton ($H = V = 29 \mu\text{m}$), and (c,d) generation of a surface soliton at a phase slip ($H = 40 \mu\text{m}$ and $V = 25 \mu\text{m}$). Excited waveguides are marked with white circles; phase slips are marked by dashed lines.

waveguides, as shown in Fig. 5(a). For low input power, we excite one of the linear guided modes of this phase slip waveguides (not shown), that undergoes symmetry breaking for larger powers and transforms into an asymmetric 1D stripe soliton, as shown in Fig. 5(a) for 1700 kW. Increasing the input power further, we observe a sharp crossover between 1D and 2D localization and the generation of a 2D soliton, see Fig. 5(b).

The generation of a 2D asymmetric nonlinear mode at the intersection of two phase-slips ($H = V = 29 \mu\text{m}$) is shown in Fig. 6(a,b). Even at relatively large power (1400 kW), the light diffracts across a quarter of the lattice [Fig. 6(a)], but for higher powers (2500 kW) the mode becomes localized eventually [Fig. 6(b)].

An example for nonlinear surface mode is presented in Fig. 6(c,d) for a single phase-slip waveguide, $H = 40 \mu\text{m}$ and $V = 25 \mu\text{m}$. For lower powers (75 kW), the light is repelled by the surface [Fig. 6(c)]. This behavior is very similar to the light propagation in one-dimensional waveguide arrays [17]. However, when the input power exceeds a threshold (2800 kW), we observe the generation of a localized state at the surface [Fig. 6(d)].

In conclusion, we have studied experimentally the generation of spatially localized modes at phase-slip waveguides and their intersections. We have generated both discrete bulk and surface solitons near the lattice structural defects, in a qualitative agreement with earlier theoretical predictions. We have also observed an interplay between the effectively 1D and 2D dynamics.

This work was supported by the Leopoldina-German Academy of Science (grant LPDS 2009-13), Fondecyt (grant 1080374), Programa de Financiamiento Basal de Conicyt (grant FB0824/2008), Deutsche Forschungsgemeinschaft (Leibniz program), and by the Australian Research Council.

[1] See, e.g., D.N. Christodoulides, F. Lederer, and Y. Silberberg, *Nature* **424**, 817 (2003).
 [2] D. Christodoulides and R. Joseph, *Opt. Lett.* **13**, 794 (1988).
 [3] W. Krolikowski and Yu.S. Kivshar, *J. Opt. Soc. Am. B* **13**, 876 (1996).
 [4] R. Morandotti, H.S. Eisenberg, D. Mandelik, Y. Silberberg, D. Modotto, M. Sorel, C.R. Stanley, and J.S. Aitchison, *Opt. Lett.* **28**, 834 (2003).

[5] H. Trompeter, U. Peschel, T. Pertsch, F. Lederer, U. Streppel, D. Michaelis, and A. Bräuer, *Opt. Express* **11**, 3404 (2003).
 [6] Yu.S. Kivshar, *Phys. Rev. B* **47**, 11167 (1993).
 [7] A.A. Sukhorukov and Yu.S. Kivshar, *Phys. Rev. Lett.* **87**, 083901 (2001).
 [8] F. Fedele, J. Yang, and Z. Chen, *Opt. Lett.* **30**, 1506 (2005).
 [9] X. Wang, J. Young, Z. Chen, D. Weinstein and J. Yang.

- Opt. Express **14**, 7362 (2006).
- [10] A. Szameit, Y. V. Kartashov, M. Heinrich, F. Dreisow, T. Pertsch, S. Nolte, A. Tünnermann, F. Lederer, V. A. Vysloukh, and L. Torner, Opt. Lett. **34**, 797 (2009).
- [11] M.I. Molina and Yu.S. Kivshar, Opt. Lett. **33**, 917 (2008).
- [12] M.I. Molina and Yu.S. Kivshar, Phys. Rev. A **80**, 063812 (2009).
- [13] V.M. Apalkov and M.E. Raikh, Phys. Rev. Lett. **90**, 253901 (2003).
- [14] K. Itoh, W. Watanabe, S. Nolte, and C. Schaffer, MRS Bull. **31**, 620 (2006).
- [15] A. Szameit, J. Burghoff, T. Pertsch, S. Nolte, and A. Tünnermann, Opt. Express **14**, 6055 (2006).
- [16] J.W. Fleischer, M. Segev, N.K. Efremidis, and D.N. Christodoulides, Nature **422**, 147 (2003).
- [17] S. Suntsov, K.G. Makris, D.N. Christodoulides, G.I. Stegeman, A. Natché, R. Morandotti, H. Yang, G. Salamo, and M. Sorel, Phys. Rev. Lett. **96**, 063901 (2006); C.R. Rosberg, D.N. Neshev, W. Krolikowski, A. Mitchell, R.A. Vicencio, M.I. Molina, and Yu.S. Kivshar, Phys. Rev. Lett. **97**, 083901 (2006).